Građevinski materijali i konstrukcije
Building Materials and Structures
journal homepage: www.dimk.rs

https://doi.org./10.5937/GRMK2400008M

**Original scientific paper**

# Experimental investigation of bearing capacity of 3D printed concrete segmental girder

Stefan Ž. Mitrović[*1)], Ivan Ignjatović[2)]

[1)] *University of Belgrade, Faculty of Civil Engineering, Bulevar kralja Aleksandra 73, 11000, Belgrade, Serbia. ORCID 0000-0001-7254-6860*
[2)] *University of Belgrade, Faculty of Civil Engineering, Bulevar kralja Aleksandra 73, 11000, Belgrade, Serbia. ORCID 0000-0002-2679-0982*

*Article history*
*Received:* 20 August 2024
*Received in revised form:* 04 September 2024
*Accepted:* 08 September 2024
*Available online:* 20 September 2024

*Keywords*
3D printed concrete,
segmental beam,
connections,
prestressing,
bearing capacity

*ABSTRACT*

3D concrete printing (3DCP) technology represents a new approach to producing contemporary concrete structures. The application of sophisticated equipment such as a 3D printer has brought numerous advantages, which were noted through significant practical application. Currently, 3DCP technology is being developed in two main directions: on-site production of entire structures and prefabricated construction. However, 3DCP technology has not yet reached its full potential in prefabrication as the connections between individual segments and their capacities under horizontal and vertical loads, have not yet been extensively investigated. This paper focuses on the experimental testing of the bearing capacity of a beam constructed by connecting individual segments of 3D printed concrete. The segments are connected using post-tensioning steel bars. The experimental program included testing a single segment as well as a segmental girder in a 3-point test. In the case of the individual segment, failure occurred due to the loss of tensile capacity of the concrete. For the segmental beam, failure occurred when the shear capacity was reached. Shear fracture was accompanied by diagonal cracks extending from the point of force application towards the beam supports.

## 1 Introduction

The construction industry has a significant impact on the gross domestic product (GDP) of each country, not only through construction activities but also through related industries such as mechanical engineering, electrical engineering, material production, and others. Over the centuries, the construction industry has undergone constant changes and innovations driven by advancements in science and technology. However, compared to other sectors, construction has experienced a relativelely slow increase in productivity. One potential direction for enhancing productivity development in this sector is the application of 3D concrete printing technology (3DCP). The digitalisation of the building process significantly reduces the time required for construction, material waste, and errors [1]–[3].

3D printing technology is a modern method for creating three-dimensional shapes. It originated as a laboratory technique, with one of the pioneers being Chuck Hull, who successfully printed the first three-dimensional shape in 1986. [4]. The concept of 3D printing can be applied to a variety of materials, such as plastic, composite, concrete or steel. Behroh Hoshnevis from the University of Southern California patented the Contour Crafting (CC) method for 3DCP in the late 20th century [5]–[7] which has since become the most widely used method for concrete printing.

In addition to CC technology, two other methods have been developed and used for 3D concrete printing (3DCP): the Inject Printing method and the Shotcrete 3D Printing (SC3DP) technology [7]–[10].

3DCP using the aforementioned methods has been successfully implemented in various applications, as shown in Figures 1-3:

1. Individual elements, such as columns and walls
2. Decorative elements, including arabesques, ornaments, and facade panels
3. Outdoor furniture, such as benches, tables, and planters
4. Sculptures and monuments
5. Single-story and multi-story buildings, including family houses and residential buildings
6. Pedestrian bridges and similar structures

It is important to note that companies specializing in material production, such as Lafarge and Sika, have recognized 3DCP technology as a new construction method. Ready-made premixes for use in 3D printing are now available on the market. Companies like COBOD BOD2, Apis Cor, Contour Crafting, and XtreeE have developed printers capable of printing large structures, including one-story houses, on-site [11]. Support for these projects has been provided by companies specializing in formwork, such as PERI and DOKA [12].

* Corresponding author:
*E-mail address:* smitrovic@imk.grf.bg.ac.rs

Figure 1. Two-story Beckum house [13]

Figure 2. Striatus bridge [13]

Figure 3. Horizontally printed panel [1]

The advantages of using 3D printing technology in the production of contemporary concrete structures are numerous [13]. First of all, significant time savings are achieved because the process is automated, reducing the need for labor. A 3D printer requires only a small number of operators. Additionally, 3D printing technology allows for greater freedom in the design of elements and structures. There is no need for complicated formwork, which is often difficult to create for more complex elements and can only be used once [11]. The cost of construction is reduced, as the value of the formwork typically accounts for about 35–60% of the element's price [15]. Furthermore, material waste and construction waste on-site can be minimized. It is also possible to use "green" concrete by incorporating recycled or waste materials [14], [16]. The application of 3D concrete printing enhances workplace safety, reduces human errors and omissions, and is suitable for use in challenging conditions. This technology is particularly well-suited for constructing buildings intended for rapid accommodation following natural disasters such as earthquakes and floods. These structures can also be used to house refugees or patients during pandemics like COVID-19.

There are also some shortcomings and open questions regarding the broader practical application of this technology [17]. A 3D printer is a sophisticated piece of equipment that requires a substantial initial investment, which can hinder the wider adoption of this method, as low cost and simple production are the main reasons for the widespread use of concrete in construction. Additionally, the operator must be adequately qualified. To print an entire structure, a printer larger than the structure itself is required, leading to complex and costly printer construction [18], [19]. Thus, the authors believe that 3DCP technology needs to be adapted for the prefabrication of concrete elements. In such cases, individual segments are produced in a prefabrication plant, transported to the construction site, and then assembled. Challenges include ensuring proper connections between segments, addressing cold joints, and incorporating reinforcement, if needed. A significant obstacle to the wider application of this technology is the inability to achieve consistent quality of printed concrete using the same mixture on different printers. Therefore, the quality of the final product depends on the correlation between the mixture and the printer, as demonstrated in an interlaboratory test conducted by the University of Eindhoven and the University of Delft [20]. The incorporation of reinforcement remains an open question, although various models have been proposed [21]. The development of an adequate and robust static system for safely transmitting loads in 3DCP structures is still unresolved. Additionally, there are currently no material models for the static and dynamic calculation of structures [12], [22].

The scientific community has recognized the open questions and obstacles related to 3DCP technology. The RILEM organization, through its two technical committees, TC 276-DFC and TC 304-ADC, is addressing the issue of standardizing the 3DCP process and laboratory testing of the properties of 3D printed concrete. Namely, there are currently no standardized models or guidelines for the design and calculation of materials and elements, including standards and regulations for the production of fresh concrete mix, testing properties in both fresh and hardened states, the 3D printing process, and the testing of finished elements and structures. Additionally, committees such as ACI Committee 564, ISO/TC 261, and ASTM Committee F42 have been established to focus on these challenges. The preliminary version of the new edition of standard EN 206-4, which pertains to 3DCP technology, is expected to be released in 2027 [12].

The aim of this paper was to analyse the current state-of-the-art in the field of experimental testing of segmental concrete elements produced using 3DCP. Additionally, the paper presents the authors' own experimental results from the initial phase of producing and testing a prototype of precast 3DCP two-segment girder.

## 2 3D printed concrete segmental elements: state-of-the-art

As mentioned in the previous chapter, prefabrication holds significant potential for the further development of 3D concrete printing technology. Open questions include the manufacturing of connections and the verification of the load-bearing capacity and serviceability of the elements [12], [21]. The first elements that were manufactured and analyzed as segmental components are beams. In addition to being printed as a single piece, beams can also be constructed by connecting smaller individual segments using epoxy adhesives, reinforcement, or post-tensioning. The tests conducted focused on determining the bending or shear capacity of the beams [12]. A summary of the tests from the literature review is presented in Table 1, showing the types of elements and tests performed, the type and content of fibers, and the type of reinforcement or cables used. An example of these tests is shown in Figure 4.

*Table 1. Experimental and numerical analysing of 3DCP segmental beams and bridges*

| Ref. | Type of element | No | Dimension of elements [mm] | Type of test | Type of fibers | Content of fibers [%] | Reinforcement | Type of reinforcement | Cables | Type of cables | FEM Analysis |
|---|---|---|---|---|---|---|---|---|---|---|---|
| [23] | Bridge (segmental) | 1 | 1720x460x500 | 4-point bending | PP | - | Cable (added by printer nozzle) | High-strength steel cable Ø 0.63 mm | Post tensioning | 9 Dywidag-system tendons (Ø15.7 mm, Y1860 steel grade), initial load 120 kN | Yes |
| | Bridge (segmental) | 1 | 3440x920x6500 | Live load/reached 100% of SLS Moment in span | PP | - | Cable (added by printer nozzle) | High-strength steel cable Ø 0.63 mm | Post tensioning | 16 Dywidag-system tendons (Ø15.7 mm, Y1860 steel grade), initial load 150 kN | Yes |
| [24] | Beam (segmental) | 1 | 200x450x3000 | 3-point bending | PP | 0.50 | Manually placed | Steel rebar Ø 16 mm | / | / | SAP2000 |
| [25] | Beam (segmental) | 7 | 240x240x960 | 3-point bending | / | / | Manually placed | Standard bar Ø 14 mm Stirrup Ø 8 mm (e= 80 mm) | / | / | No |
| [26] | Beam (segmental) | 1 | 4000 (span) | Bending under uniformly disturbed load | / | / | Manually placed | Steel rebar Ø 12 mm | Post tensioning | Ø 9.4 mm | Fusion 360 |
| [27] | Beam (segmental) | 1 | 2500 (span) | 4-point bending | Glass | - | / | / | Post tensioning | - | Grasshopper Robot Studio |
| [28] | Beam (segmental) | 13 | 128x216x3300 | 3-point bending | / | / | Manually placed | Standard bar Ø 12, 16, 25 mm | / | / | Abaqus |
| [29] | Bridge (segmental) | 1 | 16000 (span) | In situ | / | / | / | / | / | / | compas_3dec Sofistik |
| [30] | Beam (segmental) | 4 | 150x350x3200 | 4-point bending | / | / | Manually placed | Standard bar Ø 8,10, 12 mm Steel spirals Ø 8 mm (e= 200 mm) | / | / | No |

*Figure 4. In situ testing of the bridge with water-filled containers [23]*

The tests presented in Table 1 include the measured displacement of bridges or girders under load. Two approaches are usually used to design 3D printed concrete elements: topology optimization and the trial-and-error approach. The main goal of the presented research was to achieve the minimum required amount of material and to demonstrate the potential of 3DCP technology in prefabricated construction. In all cases, the bridges or beam girders had hollow configurations with various types of fillings. Some researchers incorporated fibers into the fresh concrete mixture. It is found that while a great range of element shapes can be created, but tensile strain in concrete cannot be completely eliminated, which is resulted that post-tensioning cables or reinforcement are required. The procedure for incorporation of cables or rebars is the same as that of conventionally made concrete elements, also with the need for filling the joints with injection mortar.

## 3 Experimental investigation

### 3.1 Scope of the experimental programme

The experimental phase of this research was divided into two main directions:

1. Determination of the bearing capacity of a single segment made of 3D printed concrete, with dimensions of 435x240x300 mm, using a 3-point test.
2. Determination of the bearing capacity of a two-segment girder created by connecting two individual segments of 3D printed concrete. The total dimensions of the girder were 435x240x600 mm, and it was tested using a 3-point test.

### 3.2 Preparation of samples

The individual segments were produced using 3D concrete printing technology, as shown in Figures 5 and 6. A 3D printer at the Faculty of Civil Engineering at the University of Belgrade was employed for this purpose [12]. The fresh concrete mixture was made using a ready-to-use, one-component premix with the commercial name Sikacrete®-751 3D, manufactured by Sika [31]. Each segment consisted of 20 layers, with an average layer height of 15 mm. The printing parameters included a printing speed of 1200 mm/min, a nozzle offset of 15 mm, and a pump pressure of 4 bar. The segments, which had a hollow lattice filling and dimensions of 435x240x300 mm, were cured in a dry environment for 28 days.

The beam is manufactured by connecting two individual segments using post-tensioning with two M16 steel bars of quality 8.8, as shown in Figures 7 and 8. The bars are centrally placed through the hollow structure of the segments. Steel plates with dimensions of 500x300x10 mm, along with additional plates, are positioned at the ends of the segments. These steel plates are adhered to the segments using epoxy paste adhesive. The connection of the segments is achieved through post-tensioning. The segments are in dry contact with each other. The steel bars are tightened to the required level using a torque wrench. GEOKON Model 4000 vibrating wire strain gauge sensors (VWSG) were installed on the segments prior to connecting them.

*Figure 5. The process of 3DCP of individual segments*

*Figure 6. Printed individual segments*

*Figure 7. Individual segments before connection*

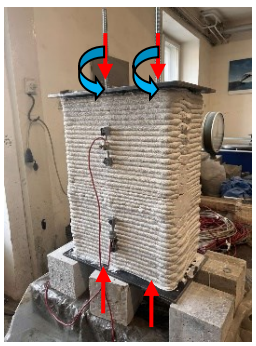

*Figure 8. The post-tensioning including the tightening of nuts with a torque wrench*

The purpose of the post-tensioning force is to connect the segments into a single element and to ensure the required shear capacity of the beam. The beam, with a span-to-height ratio of less than three, supposed to exhibit shear failure in the 3-point test. The criterion for selecting the prestressing force was based on the contribution of the normal force to the shear capacity of the beam, as outlined in Eurocode 2 [32], through the parameter $\sigma_{cp}$. The post-tensioning force was determined by limiting the parameter $\sigma_{cp}$ to a value of $0.2*f_{cd}$, where $f_{cd}$ represents the design compressive strength of the concrete. The required force was calculated based on a cross-sectional area of 59712 mm² and concrete class C25/30, resulting in a value of 160 kN, or 80 kN per steel bar. The maximum permissible force in a bar of quality 8.8 is 90 kN. To achieve the necessary post-tensioning forces, each bar had to be tightened with a torque of 192 Nm.

The strain of the beam during post-tensioning was measured by means of vibration wire strain gauges (VWSG). The normal force induced in the girder is calculated as the product of the modulus of elasticity, the cross-sectional area, and the mean value of the measured strain. The testing of the modulus of elasticity was performed on two types of samples: mold-cast samples and printed samples. In both cases, the modulus of elasticity exhibited a value of 27 GPa. The nut tightening was performed in several stages. The values of the measured strains are presented in Table 2, along with the difference between the measured force and the expected force based on theoretical calculations. On the first day of post-tensioning, the beam was prestressed and then unloaded to allow for necessary adjustments and fitting of the segments. Final post-tensioning was carried out the following day, after which the beam was subjected to a 3-point test until failure.

### 3.3 Testing of the individual segment

The first part of the experimental program focused on testing an individual segment without reinforcement or steel fibers using a 3-point test. The experimental setup is illustrated in Figure 9. The segment was supported and subjected to force using steel plates, which were adhered to the segment with epoxy paste adhesive. The segment was positioned on fixed and roller supports, with a span of 240 mm. The test was conducted using an Amsler press with a capacity of 2500 kN.

The load was applied gradually to the sample at a rate of 1 kN/sec until failure occurred. This setup allowed for the evaluation of the segment's bending capacity and the determination of its structural performance under load.

The ultimate load capacity of the segment was 130 kN, and the total test duration was 2.50 minutes. The fracture pattern observed in the individual segment after reaching its bearing capacity is depicted in Figures 10 and 11.

*Table 2. Measured strain in the post-tensioning process of segmental beam*

| First day – 16/07/2024 | | | | | | | | |
|---|---|---|---|---|---|---|---|---|
| Torque [Nm] | Expected Force by bar [kN] | Total expected force [kN] | VWSG 1 [με] | VWSG 2 [με] | VWSG 3 [με] | VWSG 4 [με] | Main value [με] | Measured force [kN] |
| 0 | 0 | 0 | 0 | 0 | 0 | 0 | 0 | 0 |
| 60 | 25 | 50 | -12 | -28 | -33 | -8 | -20 | 33 |
| 110 | 46 | 92 | -18 | -33 | -45 | -10 | -27 | 43 |
| 160 | 67 | 133 | -26 | -44 | -62 | -13 | -36 | 59 |
| 190 | 79 | 158 | -31 | -50 | -72 | -15 | -42 | 68 |
| 0 | 0 | 0 | -1 | -9 | -2 | 2 | -2 | 4 |
| Second day – 17/07/2024 | | | | | | | | |
| Torque [Nm] | Force by bar [kN] | Total force [kN] | VWSG 1 [με] | VWSG 2 [με] | VWSG 3 [με] | VWSG 4 [με] | Main value [με] | Measured force [kN] |
| 0 | 0 | 0 | 0 | 0 | 0 | 0 | 0 | 0 |
| 60 | 25 | 50 | -5 | -8 | -19 | -3 | -9 | 15 |
| 110 | 46 | 92 | -10 | -16 | -35 | -7 | -17 | 28 |
| 160 | 67 | 133 | -19 | -26 | -56 | -11 | -28 | 46 |


*Figure 9. Experimental setup for 3-point test for individual segment*

*Figure 10. The failure mechanism of the segment in 3-point test - inside*

*Figure 11. The failure mechanism of the segment in 3-point test - outside*

### 3.4 Testing of the segmental girder

The segmental girder, with dimensions of 435x240x600 mm, was tested using an Amsler press with a capacity of 2500 kN. The beam underwent a 3-point test. Steel plates, adhered with epoxy paste adhesive, were used to provide support and apply force to the beam. The beam was placed on fixed and roller supports with a span of 500 mm. The experimental setup is illustrated in Figure 12.

Before the start of the test, strain values were measured using sensors and axial prestressing force was confirmed. The transversal force (P, Figure 12) was applied incrementally, with initial steps of 5 kN up to 100 kN, followed by 10 kN steps up to 200 kN, and then 20 kN steps. During testing, there were brief pauses, leading to minor force reductions attributed to sample adjustments. The total test duration was 120 minutes with obtained capacity force of 333 kN. Strain measurements were taken at each step until the

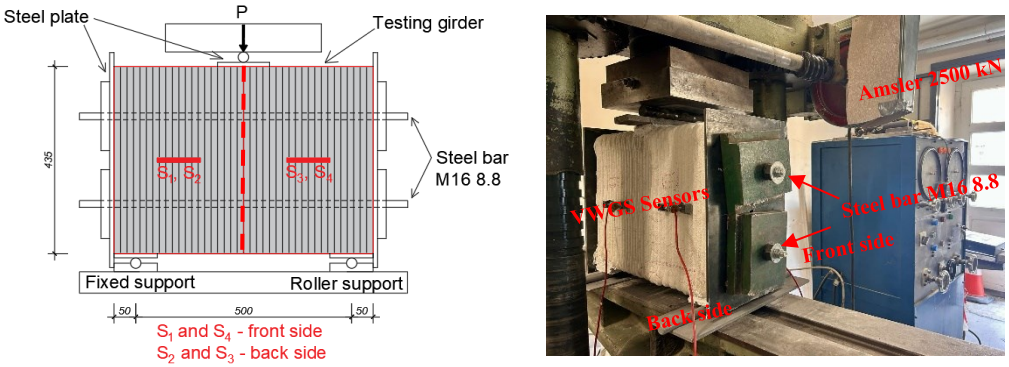


*Figure 12. Experimental setup for 3-point test for segmental beam*

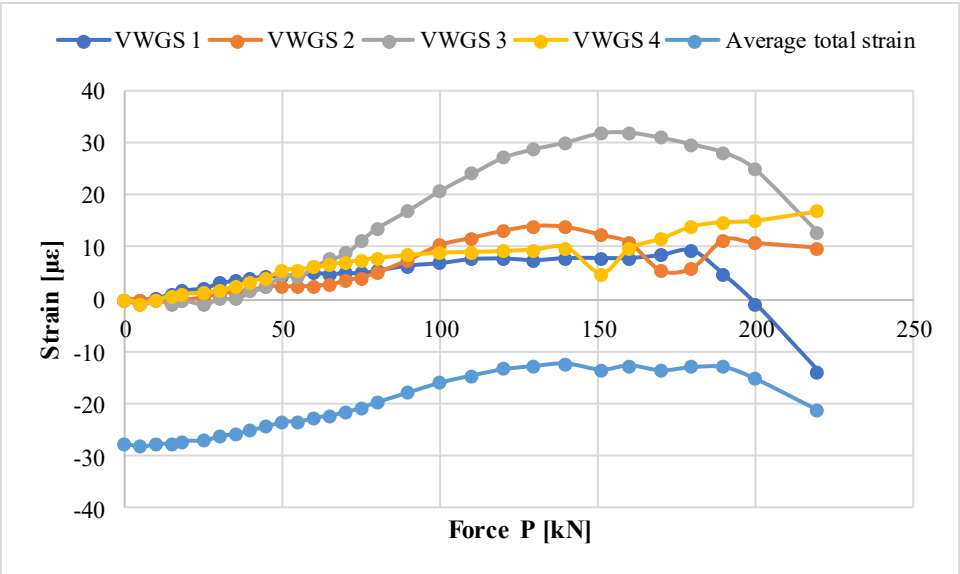


*Figure 13. Measured strains in segmental girder*

first crack appeared, at which point the sensors were removed to prevent potential damage due to the girder failure. The S1-S4 curves on Figure 13 show the strain value without previous strain from the post-tensioning phase, i.e. only strains resulted from the action of trasversal load P. The blue curves with name “Average total strain” represent the total value of strain of the middle of cross section height with added compressive strain from post-tensioning phase. Figure 14 shows the crack pattern of the segmental beam, including the force values and crack widths. The failure mechanism of the segmental beam in the 3-point bending test is illustrated in Figures 15 and 16.

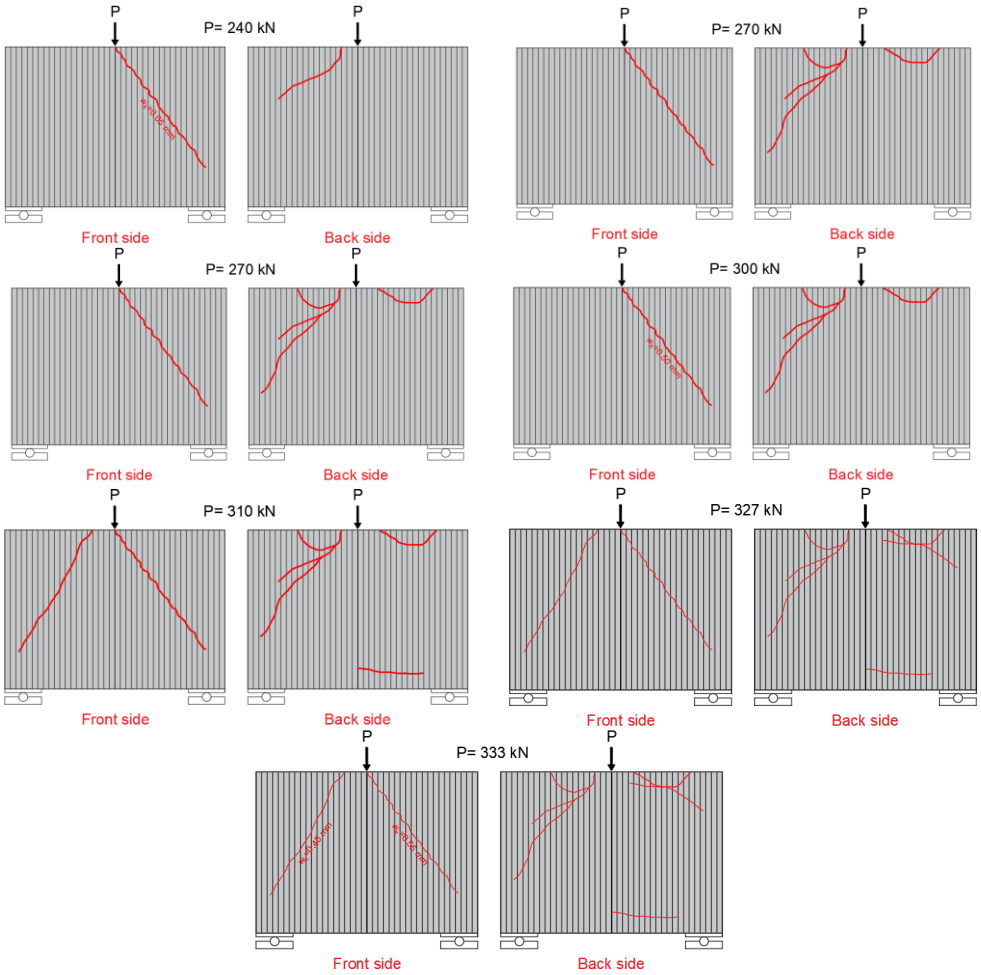


*Figures 14. Crack pattern in tested segmental beam*

*Figure 15. The failure mechanism of the segmental beam in 3-point test – front side*

*Figure 16. The failure mechanism of the segmental beam in 3-point test – back side*

### 3.5 Discusion of results

The testing of the individual segment revealed bending failure, characterized by the formation of a crack at the mid-span and its subsequent propagation along the height of the segment. This type of failure is anticipated given that the sample was manufactured without reinforcement or steel fibers. Due to the short span and the force application near the segment supports, shear capacity of tested elements was higher.

Previous research [33] determined the splitting strength. For splitting failure, the predicted capacity was 143 kN. For bending failure, the predicted capacity force was 150 kN. The prediction was based on a single calculation of stresses in the cross-section and the tensile stress limitations, which are set to the value of $f_{ctm}$ according to Eurocode 2 [32]. The experimental testing yielded a capacity force of 130 kN. The observed fracture involved a crack opening in the tensile zone, progressing through four layers and continuing between layers to the segment's top. The fracture pattern suggests adequate printing quality and high interlayer bond strength. The behavior of the printed segments is comparable to that of traditionally cast samples. The experimental capacity force is approximately 15% lower than the theoretical prediction, which is based on bending failure.

Measured strains in prestressing phase of two-segment girder testing (Table 2) indicated an eccentric application of the post-tensioning force. The presence of a bending moment around the longitudinal axis of the beam was detected, resulting from the asymmetrical stress distribution across the cross-section, particularly with high values at the edge where sensor S3 was installed. Localized damage at the corners of the segments is evident in Figure 17. The strains did not return to their initial values during the unloading process on the first day, which is likely related to this localized damage.

With a torque of 160 Nm applied to each bar, the theoretical post-tensioning force per bar was 67 kN, totaling entered force of 134 kN for the beam. However, testing revealed that the actual mean post-tensioning force was 46 kN. The difference between the entered and measured post-tensioning force may be due to eccentricity or bending of the supports, including the anchor zone. These factors will be more considered in future research. Given the beam's short span, shear failure with diagonal cracks was anticipated rather than bending failure. According to Eurocode 2 [32], the predicted shear capacity of the beam was 290 kN.

The first diagonal crack appeared at a force of 240 kN (Figure 14) on the beam's front side, detected by an unexpected change in sensor readings. This crack, initially 0.05 mm wide, propagated to 0.55 mm at a force of 333 kN. A significant force drops from 240 kN to 192 kN was observed, with the crack widening further during force application.

A second diagonal crack, symmetrical to the first, developed on the same side at a force of 310 kN, with a width of 0.45 mm at 333 kN, Figure 16. Diagonal cracks also emerged on the back side of the beam, with the first appearing at 300 kN and a second at 327 kN. The experimental testing reached a maximum capacity force of 333 kN, indicating shear failure with diagonal cracks on both sides of the beam from the force application points to the supports (Figures 15 and 16). Theoretical predictions estimated a capacity force of 290 kN, whereas the experimental results yielded 333 kN, showing a 13% difference. The diagonal cracks passed through the layers without delamination between them. Furthermore, there was no failures at the segment joints. Therefore, the connection method proved to be effective.

All sensors without previous strain in girder from post-tensioning, detected tensile strain with increasing force, except for sensor S1, which detected compressive strain after 200 kN. Sensors S1, S2, and S4 recorded similar strain values, while sensor S3 showed the highest strain values, indicating the impact of post-tensioning eccentricity on beam behavior. Sensor S3 recorded the highest strain during the post-tensioning phase. The average value of total strain on the middle of the sample height is negative during the testing, which indicate the compressive strain in that direction. It should also be noted that the experimental testing of individual segments with dry contact resulted in a noticeable gap opening during force application, as shown in Figure 18.

## 4 Conclussions

Based on the presented findings, the following conclusions can be drawn:

1. 3D concrete printing technology holds significant promise for advancing contemporary concrete structures, particularly as part of the 4.0 industrial revolution. The integration of modern software and 3D printing machines is expected to revolutionize construction practices.

2. While 3D printing facilitates the creation of intricate elements, challenges remain in designing effective connections between segments. There is a need for further research into verifying the bearing capacity of these connections and assessing the long-term performance of 3D printed elements, particularly under lateral loads.

*Figure 17. The local destruction of segments*

*Figure 18. The gap between segments*

3. Previous research confirm that post-tensioning has proven to be an effective method for connecting individual segments, enhancing both bending and shear capacities. The hollow structure of printed segments accommodates the installation of cables and reinforcement bars, addressing tensile stresses and improving structural integrity.

4. Own experimental testing of individual printed segments confirmed high print quality and good correlation between the printer and the fresh concrete mixture. The capacity force measured was in line with theoretical predictions for bended elements.

5. Post-tensioning with steel bars introduced compressive forces and provided good connection of the segments; accidental eccentricity of prestressing force caused stress concentrations and relatively small-localized damage.

6. The tested two-segments girder exhibited shear failure, as anticipated based on its span-to-height ratio and relatively high prestressing level. Failure mode and crack pattern suggests that the proposed connection approach is structurally sound. Also, this qualitative test showed the success of this assembling method and confirmed that axial forces in the beam can be achieved with steel rebars tightened with torque wrench only.

**CRediT authorship contribution statement**

**Stefan Mitrović:** Data curation, Formal Analysis, Investigation, Project administration, Resources, Validation, Visualization, Writing – original draft prepraration. **Ivan Ignjatović:** Conceptualization, Methodology, Project administration, Resources, Supervision, Validation, Writing— review and editing.

**Declaration of competing interest**

The authors declare that they have no known competing financial interests or personal relationships that could have appeared to influence the work reported in this paper.

**Acknowledgments**

The authors gratefully acknowledge the support of Nenad Zorić from SIKA Serbia, Srđan Ilić from ADING Serbia and Elko-var Valjevo which provided materials needed for experimental testing. For assistance in conducting the experimental part, the authors thank their colleagues from the Laboratory for Materials and the Laboratory for Construction Faculty of Civil Engineering University of Belgrade, Associate Professor Zoran Mišković, Siniša Savatović, Sava Stavnjak, Mladen Jović and Dragan Žderić. This research was supported by the Ministry of Science, Technological Development, and Innovation of the Republic of Serbia (grant number 2000093).

**References**

[1] R. A. Buswell, W. R. Leal de Silva, S. Z. Jones, and J. Dirrenberger, 3D printing using concrete extrusion: A roadmap for research, Cem. Concr. Res., vol. 112, no. June, 2018, 37–49, doi: 10.1016/j.cemconres.2018.05.006.

[2] N. Labonnote, A. Rønnquist, B. Manum, and P. Rüther, Additive construction: State-of-the-art, challenges and opportunities, Autom. Constr., vol. 72, 2016, 347–366, doi: 10.1016/j.autcon.2016.08.026.

[3] S. Marinković, "Concrete structures in the 21 st century and further," Civ. Eng. 2021 Achiev. Visions, 2021, pp. 2–17.

[4] N. Shahrubudin, T. C. Lee, and R. Ramlan, An overview on 3D printing technology: Technological, materials, and applications, Procedia Manuf., vol. 35, 2019,1286–1296, doi: 10.1016/j.promfg.2019.06.089.

[5] B. Khoshnevis, Automated construction by contour crafting - Related robotics and information technologies, Autom. Constr., vol. 13, no. 1, 2004, 5–19, doi: 10.1016/j.autcon.2003.08.012.

[6] B. Zareiyan and B. Khoshnevis, Effects of interlocking on interlayer adhesion and strength of structures in 3D printing of concrete, Autom. Constr., vol. 83, 2017, 212–221, doi: 10.1016/j.autcon.2017.08.019.

[7] O. Bukvić, V. Radonjanin, M. Malešev, and M. Laban, Basic fresh-state properties of extrusion-based 3D printed concrete, Gradjevinski Mater. i Konstr., vol. 63, no. 4, 2020, 99–117, doi: 10.5937/grmk2004099b.

[8] F. Heidarnezhad and Q. Zhang, Shotcrete based 3D concrete printing: State of art, challenges, and opportunities, Constr. Build. Mater., vol. 323, no. January, 2022, 126545, doi: 10.1016/j.conbuildmat.2022.126545.

[9] D. Lowke, E. Dini, A. Perrot, D. Weger, C. Gehlen, and B. Dillenburger, Particle-bed 3D printing in concrete construction – Possibilities and challenges, Cem. Concr. Res., vol. 112, no. November 2017, 2018, doi: 10.1016/j.cemconres.2018.05.018.

[10] P. Shakor, S. Nejadi, G. Paul, and J. Sanjayan, A Novel Methodology of Powder-based Cementitious Materials in 3D Inkjet Printing for Construction Applications, *6th Int. Conf. Durab. Concr. Struct. ICDCS 2018*, no. July, pp. 685–695, 2018.

[11] I. Ignjatović, S. Mitrović, J. Dragaš, and V. Carević, Structural application of 3D concrete printing technology, in *Proceedings 16th International Congress of Association of Structural Engineers of Serbia 2022*, 2022, no. October, pp. 458–469.

[12] I. Ignjatović, J. Dragaš, S. Mitrović, and M. Vidović, 3D ŠTAMPANI BETONI U SRBIJI – REALNOST ILI DALEKA BUDUĆNOST?, in *Zbornik radova Naučno-stručni skup "'Aktuelni trendovi u oblasti građevinskih materijala i konstrukcija'", Beograd, 10. maj 2024. godine, 2024*, 2024, no. May, pp. 16–30, doi: 10.46793/diimk24.016ii.

[13] F. Bos, R. Wolfs, Z. Ahmed, and T. Salet, Additive manufacturing of concrete in construction: potentials and challenges of 3D concrete printing, Virtual Phys. Prototyp., vol. 11, no. 3, 2016, 209–225, doi: 10.1080/17452759.2016.1209867.

[14] P. Feng, X. Meng, J. F. Chen, and L. Ye, Mechanical properties of structures 3D printed with cementitious powders, Constr. Build. Mater., vol. 93, 2015, 486–497, doi: 10.1016/j.conbuildmat.2015.05.132.

[15] A. Perrot, D. Rangeard, and A. Pierre, Structural built-up of cement-based materials used for 3D-printing extrusion techniques, Mater. Struct. Constr., vol. 49, no. 4, 2016, 1213–1220, doi: 10.1617/s11527-015-0571-0.

[16] K. Kanishka and B. Acherjee, Revolutionizing manufacturing: A comprehensive overview of additive manufacturing processes, materials, developments, and challenges, J. Manuf. Process., vol. 107, no. October, 2023, 574–619, doi: 10.1016/j.jmapro.2023.10.024.

[17] L. Gebhard, L. Esposito, C. Menna, and J. Mata-Falcón, Inter-laboratory study on the influence of 3D concrete printing set-ups on the bond behaviour of various reinforcements, Cem. Concr. Compos., vol.

133, no. March, 2022, doi: 10.1016/j.cemconcomp.2022.104660.
[18] D. Avrutis, A. Nazari, and J. G. Sanjayan, Industrial Adoption of 3D Concrete Printing in the Australian Market, no. Cc. Elsevier Inc., 2019.
[19] S. L. and Z. Q. Lyu Fuyan, Zhao Dongliang , Hou Xiaohui, Applied Sciences Overview of the Development of 3D-Printing Concrete, Applie Sci., 2021.
[20] S. C. F. A. L. van O. K. Nefs, E. Schlangen, T. A. M. Salet, B. Šavija, A. S. J. Suiker, and F. P. Bos, Quality Assessment of Printable Strain Hardening Cementitious Composites Manufactured in Two Different Printing Facilities, in *Second RILEM International Conference on Concrete and Digital Fabrication*, 2020, pp. 824–838, doi: 10.1007/978-3-030-49916-7_81.
[21] V. Mechtcherine et al., A roadmap for quality control of hardening and hardened printed concrete, Cem. Concr. Res., vol. 157, no. March, 2022, 106800, doi: 10.1016/j.cemconres.2022.106800.
[22] P. Narjabadifam, S. Mollaei, F. Noroozinejad, and S. Talebi, Numerical analysis of seismic behavior of an arched-roof 3D-Printed building, Gradjevinski Mater. i Konstr., vol. 67, no. 1, 2024, 1–15, doi: 10.5937/grmk2300014p.
[23] T. A. M. Salet, Z. Y. Ahmed, F. P. Bos, and H. L. M. Laagland, Design of a 3D printed concrete bridge by testing, Virtual Phys. Prototyp., vol. 13, no. 3, 2018, 222–236, doi: 10.1080/17452759.2018.1476064.
[24] D. Asprone, F. Auricchio, C. Menna, and V. Mercuri, 3D printing of reinforced concrete elements: Technology and design approach, Constr. Build. Mater., vol. 165, 2018, 218–231, doi: 10.1016/j.conbuildmat.2018.01.018.
[25] J. J. Assaad, A. A. Yassin, F. Alsakka, and F. Hamzeh, A modular approach for steel reinforcing of 3D printed concrete-preliminary study, Sustain., vol. 12, no. 10, 2020, 1–18, 2020, doi: 10.3390/SU12104062.
[26] G. Vantyghem, W. De Corte, E. Shakour, and O. Amir, 3D printing of a post-tensioned concrete girder designed by topology optimization, Autom. Constr., vol. 112, no. January, 2020, 103084, doi: 10.1016/j.autcon.2020.103084.
[27] Marc-Patrick Pfleger, S. Geyer, C. Hölzl, and M. Vill, Investigations to Improve the Carbon Footprint of Thin Walled Concrete Structures by 3D Printing Prefabricated Elements, in *International RILEM Conference on Synergising Expertise towards Sustainability and Robustness of Cement-based Materials and Concrete Structures, SynerCrete'23 - Volume 2*, 2023, pp. 653–664.
[28] A. Aramburu, I. Calderon-Uriszar-Aldaca, and I. Puente, Parametric modelling of 3D printed concrete segmental beams with rebars under bending moments, Case Stud. Constr. Mater., vol. 18, no. December 2022, 2023, e01910, doi: 10.1016/j.cscm.2023.e01910.
[29] A. Dell'Endice, S. Bouten, T. Van Mele, and P. Block, Structural design and engineering of Striatus, an unreinforced 3D-concrete-printed masonry arch bridge, Eng. Struct., vol. 292, no. July, 2023, 116534, doi: 10.1016/j.engstruct.2023.116534.
[30] S. Maitenaz, R. Mesnil, A. Feraille, and J. F. Caron, Materialising structural optimisation of reinforced concrete beams through digital fabrication, Structures, vol. 59, no. October 2023, 2024, 105644, doi: 10.1016/j.istruc.2023.105644.
[31] Sika, "Sikacrete®-751/-752 3D one-component micro-concrete for 3d printing," *Prod. Cat.*, 2020.
[32] European committee for standardization, "EN 1992-1-1: Eurocode 2: Design of concrete structures," *Eur. Stand.*, 2015.
[33] S. Mitrović and I. Ignjatović, Hardened properties of 3D printed concrete – experimental investigation, *20 th Symp. Maced. Assoc. Struct. Eng. Skopje, Repub. North Maced. 28-29 Sept. 2023.*, 1052–1064, 2023.